Synthesis of Arylidenehydrazinyl-4-methoxyphenylthiazole Derivatives: Docking Studies, Probing Type II Diabetes Complication Management Agents

Hasnain Mehmood[a], Tashfeen Akhtar*[a], Muhammad Haroon*[a,b], Ehsaan Tahir[a], Muhammad Ehsan[a], Simon Woodward[c], Mustapha Musa[c].

[a]Department of Chemistry, Mirpur University of Science and Technology (MUST), 10250-Mirpur (AJK) Pakistan. (Tashfeen Akhtar (tashfeenchem@must.edu.pk), Muhammad Haroon (haroon24486@gmail.com).
[b]Department of Chemistry, Government Major Muhammad Afzal Khan (Shaheed), Boys Degree College Afzalpur, Mirpur (Affiliated with Mirpur University of Science and Technology (MUST), 10250-Mirpur (AJK) Pakistan).
[c]GSK, Carbon Neutral Laboratories for Sustainable Chemistry, University Park Nottingham, NG7 2RD, United Kingdom

Dedication ((optional))

Abstract: Thiazole has been a key scaffold in antidiabetic drugs. In quest of new and more effective drugs a simple, efficient, high yielding (67-79%) and convenient synthesis of arylidenehydrazinyl-4-methoxyphenyl)thiazoles is accomplished over two steps. The synthesis involved the condensation of aryl substituted thiosemicarbazones and 2-bromo-4-methoxyacetophenone in absolute ethanol. The structures of the resulting thiazoles are in accord with their UV-Vis, FT-IR, ^{1}H-, ^{13}C-NMR and HRMS data. All compounds were evaluated for alpha(α)-amylase inhibition potential, antiglycation, antioxidant abilities and biocompatibility. The compounds library identified 2-(2-(3,4-dichlorobenzylidene)hydrazinyl)-4-(4-methoxyphenyl)thiazole as a lead molecule against α-amylase inhibition with an IC_{50} of 5.75±0.02 µM. α-Amylase inhibition is also supported by molecular docking studies against α-amylase. All the obtained thiazoles also showed promising antiglycation activity with 4-(4-methoxyphenyl)-2-(2-(2-(trifluoromethyl)benzylidene)hydrazinyl)thiazole exhibiting the best inhibition (IC_{50}= 0.383±0.001 mg/mL) compared to control. The tested compounds are also biocompatible at the concentration used *i.e.* 10 µM.

Keywords: Bioorganic chemistry• α-amylase Docking•Cyclizations•1,3-thiazoles•Antioxidannt•Antiglycation•Biological studies•

Introduction

Diabetes is globally emergent problem [1]. The International Diabetes Federation indicated 425 million active cases of diabetes in 2017 and this number is predicted to rise dramatically in next 25 years. A further 350 million people are at threat of acquiring diabetes across the globe [2]. The emergent factors responsible for the spread of diabetes are: improved life style, food habits and technological society [3]. Hence, along with improving life style there is a pressing need to discover, synthesize and modify both new and existing treatments to manage diabetes.

Biochemical processes in human body produce reactive oxygen species (ROS). High levels of these ROS species induce cellular oxidative stress, that can lead to diabetes mellitus (DM) [4, 5]. This metabolic disorder is linked with several complications including stockpiling of advanced glycated end products (AGEs) and slow wound healing associated with type 2 diabetes (T2D) [4]. This condition leads to an abnormal decrease in insulin and elevation of blood glucose (hyperglycaemia) [6]. The higher level of blood sugar induces glycation and accumulation of advanced glycation end products (AGEs). In order to mitigate the social cost of DM and improve patient care, there is a critical need to find new ways to control the deteriorating effect of the disease.

Traditionally, diabetes is treated by regulating the insulin level or glucose level in the blood through inhibiting the enzymes regulating the starch metabolism [7], thus inhibiting the process of glycation and use of antioxidants to reduce reactive oxygen species [8]. The use of herbs and natural extracts have been an effective mode of dibetes treatment [9-11]. These nature originated moities inhibit postprandial hyperglycemia, thus treat diabetes in an effecient manner. The tidious extractions and isolation processess of natural products directed the medicinal chemists to design and synthesize antidiabetic agents with higher efficacy and little side effects. In order to achieve this goal, bioactive scaffolds are explored, more specifically five membered heterocycles [12]. Among five membered heterocycles, thiazole holds special position with its versatile applications [12-14]. The extensive applications of thiazole make it a leading structure motif in drug discovery and medicinal chemistry [15].

Thiazole derivatives have been well documented as an important pharmacologically active class in treatment of diabetes [12, 16-21]. Several thiazole derivatives have been used to treat diabetes and its complications as summarised in Figure 1 [22]. The potential of hydrazinyl-thiazole derivatives in managing diabetes *via* α-amylase inhibition [22], glycation inhibition and antioxidant action (Figure 1 **D**) [23], led us to design and synthesize compounds **3a-o**. The findings of our previous studies suggested that presence of groups containing additional H-bond acceptor stabilize the enzyme-compound interaction, thus inhibits α-amylase from hydrolysing starch into glucose.

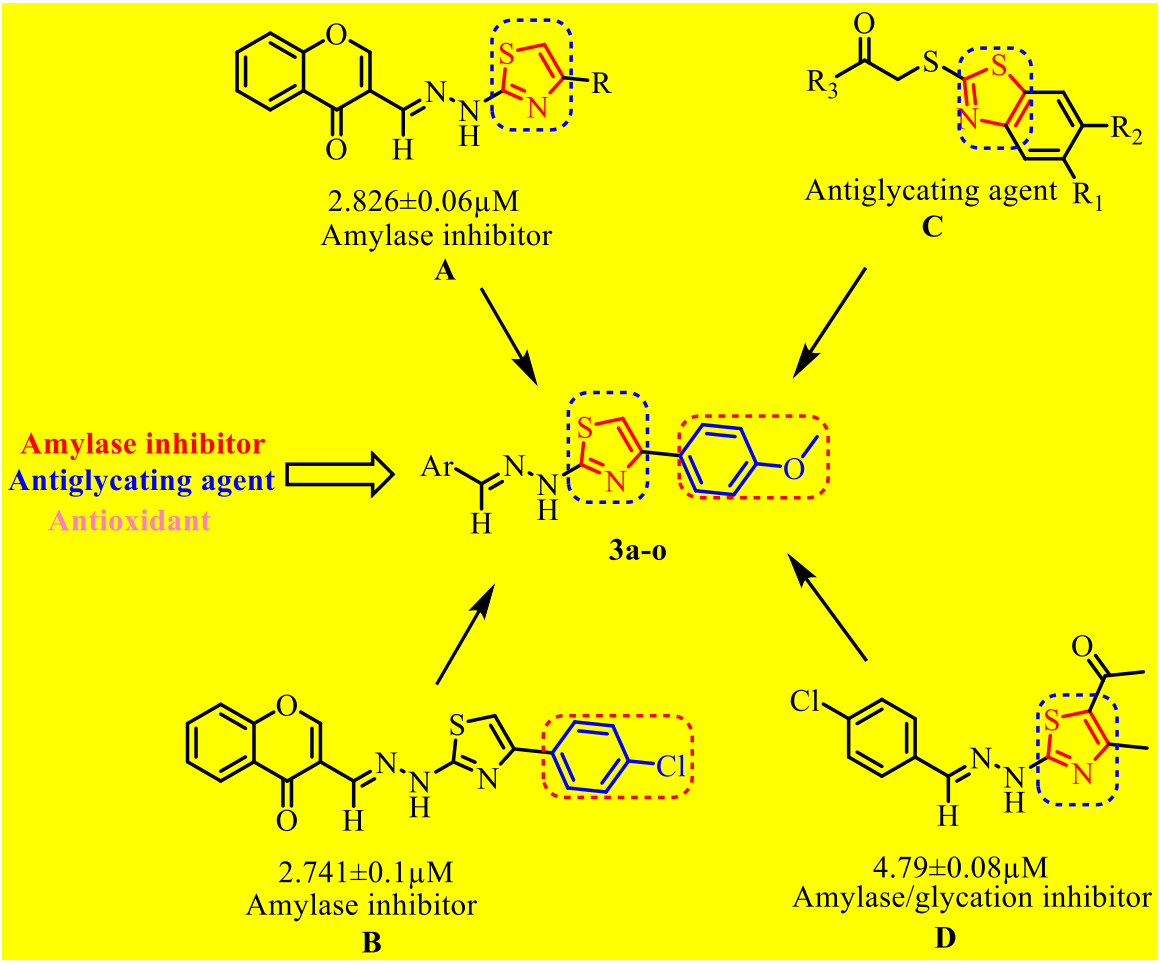

Figure 1: Rationale of the synthesis.

Results and Discussion

The compounds 2-(2-arylidenehydrazinyl)-4-(4-methoxyphenyl)thiazoles **(3a-o)** were prepared by heating an equimolar mixture of respective thiosemicarbazones [24-33] and 2-bromo-4-methoxy acetophenone in absolute ethanol as shown in Scheme 1 [34-36]. The cyclized products were achieved in moderate to good yield (67-79%).

The structures were established by spectroscopic data i.e. UV, FT-IR, ^{1}H-, ^{13}C-NMR and HRMS. In FTIR spectra of **3a-o,** absorptions at 3320-3103 cm^{-1} indicated presence of the -NH group. Additional absorption bands in the range of 2937-2918 cm^{-1} indicate aliphatic -CH stretching modes while the azomethine (-CH=N-) groups are evidenced by strong absorptions in range 1610-1550 cm^{-1}. The absorption bands in the range 1700-1421 cm^{-1} were ascribed to thiazole skeletal vibrations overlapping with aromatic ring C=C stretchings [37] and those at 1456-1313 cm^{-1} to aliphatic -CH bending vibrations. The C-O bond stretch appeared at 1132-1029 cm^{-1} while characteristic thiazole vibrations were found at 1099-705 cm^{-1} [37].

In ^{1}H-NMR spectra of **3a-o,** three proton signals as singlets at δ 2.20-2.33 ppm were ascribed to methyl group bonded to the azomethine linkage. The presence of methoxy group was similarly indicated as singlet at δ 3.73-3.86 ppm. A single uncoupled thiazole proton was observed as singlet at δ 6.39-7.23 ppm. A one proton signal as singlet at δ 7.28-8.46 ppm was attributed to the azomethine (-CH=N-) proton for all cases except **3g**. The azomethine proton in **3g** coupled to the -CF_3 moiety appeared as quartet ($^{3}J_{HF}$= 2.3 Hz). Finally, the protons in range δ 12.36-11.03 ppm were assigned to the -NH functionalities.

In their ^{13}C-NMR spectra the carbon of thiazole (C2) appeared in the range δ 166.7-170.1 ppm for all compounds (**3a-o**). Methoxy carbon signal appeared between δ 155.6-161.1 ppm while the azomethine carbon signal was observed at δ 132.3-141.9 ppm. The carbons at position 4 and 5 of thiazole appeared in range δ 145.9-151.0 and δ 98.6-102.6 ppm, respectively. The up-field carbon signals in range δ 55.3-56.2 ppm were assigned to the methoxy carbons. The synthesis of compounds was further confirmed when NMR spectra were compared with literature reported similar skeleton compounds.[38-45]

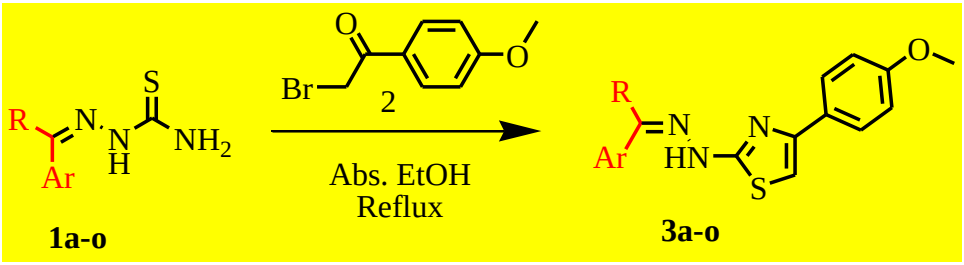

Compd.	–Ar	-R	Compd.	–Ar	-R
3a	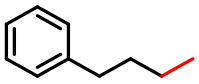	-CH_3	**3i**	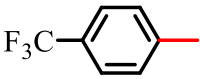	-H
3b	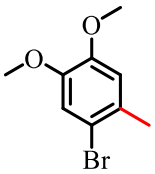	-H	**3j**	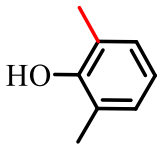	-H
3c	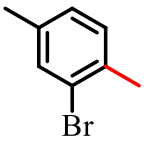	-H	**3k**	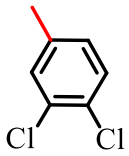	-H
3d	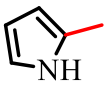	-CH_3	**3l**	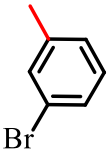	-CH_3
3e	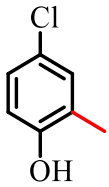	-H	**3m**	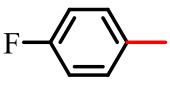	-CH_3
3f	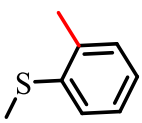	-H	**3n**	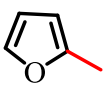	-H
3g	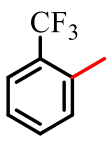	-H	**3o**	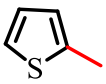	-H

3h 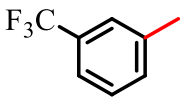 -H

Scheme 1: Synthesis of 2-(2-arylidenehydrazinyl)-4-(4-methoxyphenyl)thiazoles **(3a-o).**

After establishing the synthesis of the expected hydrazinyl-4-methoxyphenylthiazoles their biological significance was investigated by α-amylase inhibitory potential, antiglycation activity, antioxidant potential and cytotoxic behaviour by haemolytic assay.

Biological screening of 2-(2-arylidenehydrazinyl)-4-(4-methoxyphenyl)thiazoles (3a-o)

Molecular modelling study

To help understand the molecular basis of the mechanism of inhibition, molecular docking study was used to examine potential binding conformations of compounds (**3a-o**) to the active site of human pancreatic α-amylase (pdb:4W93) using Autodock Vina (See Experimental Section). Protein structure (4W93) was retrieved from Protein Data Bank (PDB) whose structure is already bound with montbretin A and a calcium ion co-factor. The bound co-crystallized ligands were removed from active pocket of protein keeping the co-factor intact to study the inhibition mechanism of the active compounds. The docked ligand protein complexes were investigated with their hydrophobic/philic bonding interaction pattern and docking score (kcal/mol). The key interactions established by the active compounds were within 5 ˚A radius to the binding site of α-amylase.

Many poses (10 different conformations) were obtained with better binding modes and interactions inside the receptor pocket. The poses with the most acceptable scores were selected.

Table 1: Docking score and α-amylase inhibitory activity of arylidenehydrazinyl-4-methoxyphenylthiazoles (**3a-o**).

Compounds	Colour of the Ligands in Sticks	Docking Score (kcal/mol)	IC_{50}(μM ± STDEV)
3a	White	-7.982	6.35 ± 0.02
3b	Light Pink	-8.292	5.90 ± 0.07
3c	Green	-7.723	7.44 ± 0.06
3d	Blue	-7.364	6.70 ± 0.02
3e	Yellow	-8.077	6.94 ± 0.06
3f	Magenta	-7.883	6.33 ± 0.11
3g	Orange	-8.017	6.22 ± 0.11
3h	Light Pink	-8.014	6.83 ± 0.06
3i	Lemon	-7.692	8.41 ± 0.18
3j	Cyan	-8.485	5.84 ± 0.07
3k	Light Orange	-8.711	5.75 ± 0.02
3l	Dark grey	-7.412	6.89 ± 0.13
3m	Black	-7.972	8.23 ± 0.88
3n	Brown	-7.47	6.19 ± 0.08
3o	Navy blue	-7.415	5.86 ± 0.03
Acarbose	Red	-7.581	5.66 ± 0.08

Most of the favored conformations occupy pocket area in domain A. All the tested compounds were clustered well inside the gorge (Figure S80) with tremendous interactions with key amino acids including Asp300, Arg195, Asp197, His299, Tyr62, Trp58, Thr163, Ala198, Trp59, Gln63, Glu233, Leu165, Leu162, His201, Lys200, Ile235, Tyr151, His101, Asp300, Val234, Glu240 and Ser199. The docking scores had little fluctuations, and the comparison depicted that all the compounds exhibited multiple binding interactions and comparable binding score due to similar basic skeleton of the ligands (Figure S81-S85). Therefore, majority of the ligands showed efficient docking energy values. By analysing docking results of the tested compounds, it was found that most of the compounds manifested close binding scores and modes compared to the standard acarbose (-7.581 Kcal/mol) Table 1. Based on the different functional groups on basic skeleton of the ligands, all compounds developed a different level of interactions, with docking score ranging from -8.711 to -7.364 Kcal/mol. Among them compound **3k** was found to be the most active and suitable scaffold for exhibiting stable binding inside the active site of the enzyme (Figure 2). This compound showed best binding energy score (-8.711 Kcal/mol) among the series of the docked compounds.

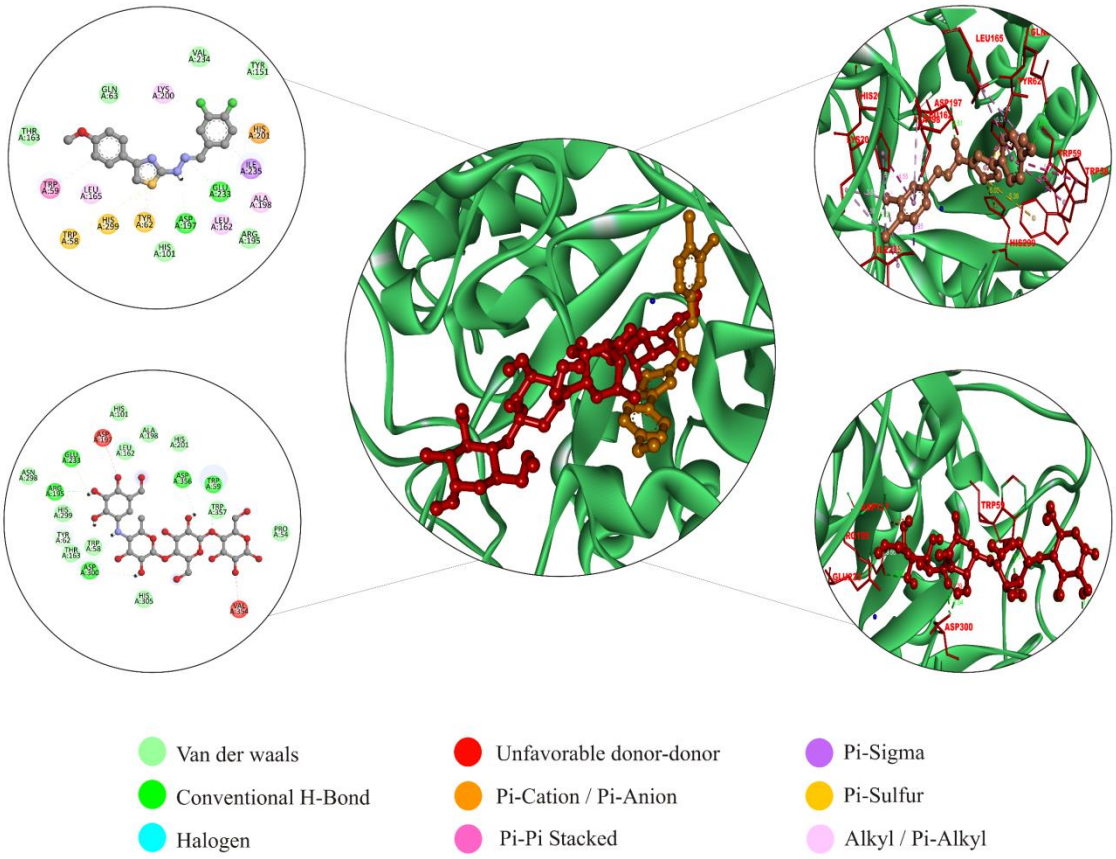

Figure 2: An overlay of the docked orientations of the most preferred conformations of compound **3k** and reference acarbose (*middle*). 2D and 3D binding interactions and positioning of the best-docked ligands with the most preferred conformations of compound **3k** in the active pocket of α-amylase (*top*) compared to the acarbose (*bottom*).

The promising score of these ligands can be attributed to the docking orientation of the most favorable conformation inside the active site gorge of the receptor (Figure 2). When we put eyes on the binding interactions of **3k**, we could reveal that it showed π-cation interactions at His201 (6.45 Å), π-sigma interactions at Ile235 (4.02 Å), π-sulfur linkages at Tyr62, His299 and Trp58 (3.07, 5.09 and 5.29 Å respectively), π-π stacking at Trp59 (5.50 Å), and π-alkyl interactions at Ala198, Leu162, Leu165 and Lys200 (5.44, 5.18, 4.74 and 3.84 Å respectively), in addition to the hydrogen bonding at (Glu233 at 3.07 Å and Asp197 at 2.61 Å). On comparison, no such π-π stacking and π -sulphur interactions were observed when acarbose is binding to the target (Figure 3). These striking interactions and binding score suggest that the compound **3k** possess the strong potential against α-amylase inhibition.

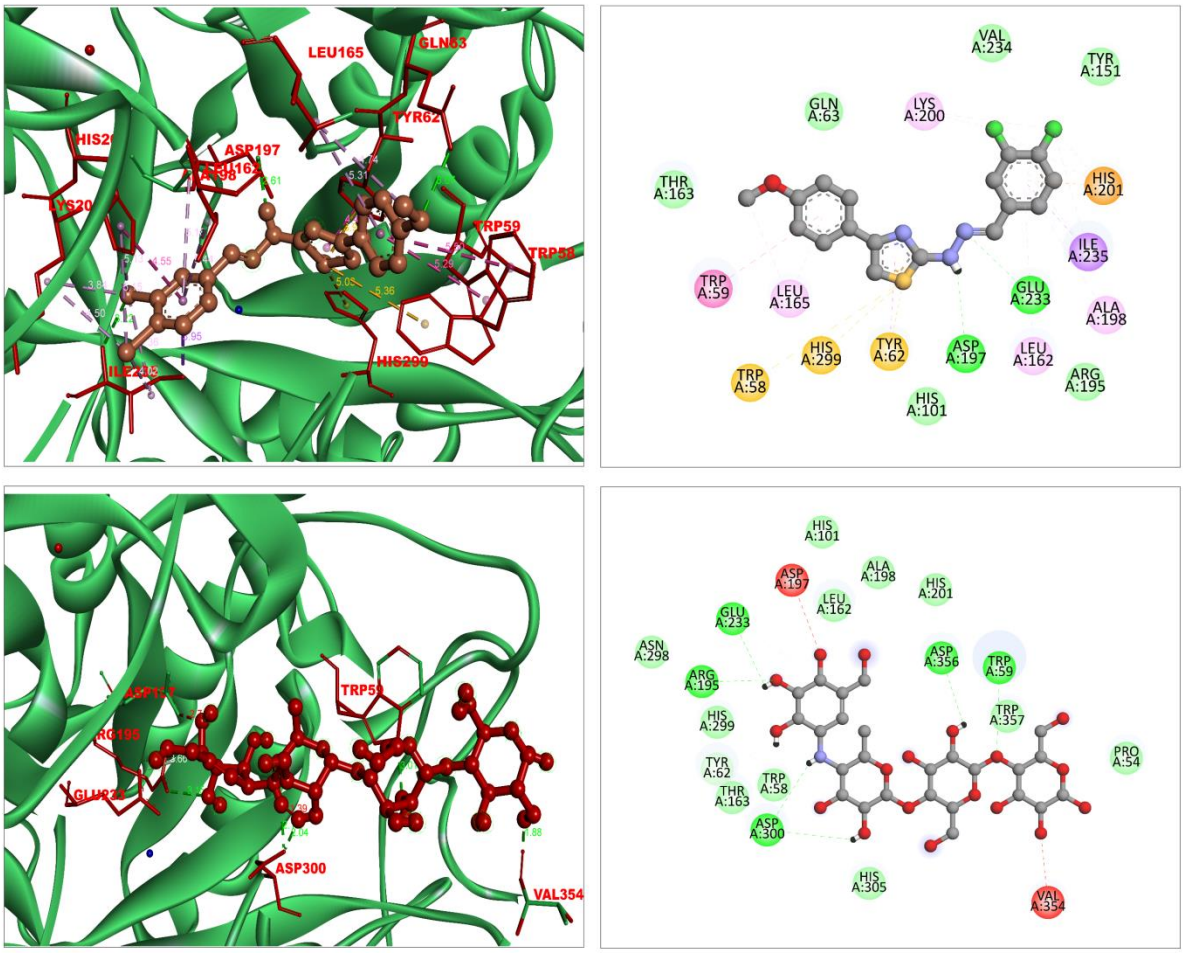

Figure 3: Ribbon (*left*) and ball and stick (*right*) illustration of the docking pose of compound **3k** (*top*) and acarbose (*bottom*).

Structure activity relationship (SAR) for α-amylase inhibition potential

The arylidenehydrazinyl-4-methoxyphenylthiazoles were screened for their α-amylase inhibition potential. Acarbose was used as reference inhibitor with an IC_{50} value 5.66±0.08 µM. The synthesized molecules possess exclusive structural features (hydrogen bond donor, hydrogen bond acceptors and hydrophobic interactions) which play their role in exhibiting α-amylase inhibition. The slight difference in α-amylase inhibition may be attributed to same skeleton and varying aryl groups as shown in Scheme 1. The results are presented in Table 2. These results revealed that compounds showed fairly moderate to good α-amylase inhibition with IC_{50} values ranging from 5.75±0.02 to 8.41±0.18 µM. Compounds, **3b** (2-bromo-4,5-dimethoxy), **3j** (2-hydroxy-3-methyl), **3k** (3,4-dichloro) and **3o** (thiophen-2-yl) showed comparable inhibition to standard. Comparing the inhibition potential of five member heterocyclic ring present as aryl group in the structure, the results revealed that thiophen-2-yl ring (**3o**) shows better inhibition (IC_{50}= 5.86±0.03 µM) than furan-2-yl (**3n**) and pyrrol-2-yl (**3d**) rings. This may be attributed to additional π-sulfur interaction leading to better stabilization of ligand-enzyme complex.

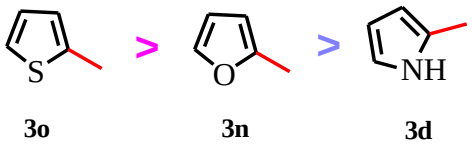

Figure 4: Decreasing order of α-amylase inhibition

The comparison of mono substituted aryl groups revealed that *ortho* substitution enhanced the inhibition potential as evidenced in compounds **3f** and **3g**. The *meta* substituted aryl group (**3h** and **3l**) showed less inhibition potential than *ortho*. The *para* substituted (**3i** and **3m**) showed least inhibition potential. The order of substitution pattern on aryl ring is shown in Figure 5.

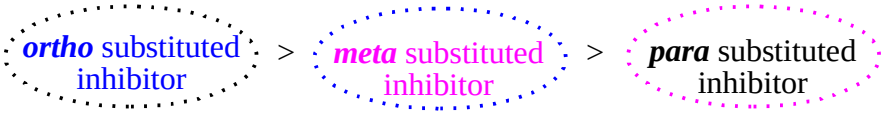

Figure 5: α-Amylase inhibition order of *ortho*, *meta* and *para* substituents.

The results also revealed that the inhibition potential is dose dependent *i.e.* inhibition potential increases with increase in dose concentration.

Table 2: Percentage α-amylase inhibition of compounds **3a-o.**

Compd.	% Age α-amylase inhibition			IC_{50}±SEM (μM)
	1 μM	5 μM	10 μM	
3a	41.60	54.96	67.65	6.35±0.02
3b	48.87	61.36	71.24	5.90±0.07
3c	39.29	46.09	57.74	7.44±0.06
3d	43.02	53.66	62.86	6.70±0.02
3e	41.26	50.46	61.50	6.94±0.06
3f	41.94	52.83	68.96	6.33±0.11
3g	42.61	55.48	69.34	6.22±0.11
3h	39.74	50.92	62.80	6.83±0.06
3i	28.76	38.70	52.72	8.41±0.18
3j	49.98	60.75	72.70	5.84±0.07
3k	52.43	62.16	73.25	5.75±0.02
3l	35.37	49.94	62.93	6.89±0.13
3m	32.13	45.15	55.90	8.23±0.88
3n	44.04	57.72	68.58	6.19±0.08
3o	47.18	61.42	72.02	5.86±0.03
Acarbose	52.39	63.18	74.46	5.66±0.08

Structure activity relationship (SAR) for anti-glycation activity

The compounds **3a-o** were evaluated for their glycation inhibitory potential using amino-guanidine as standard inhibitor (IC_{50}= 0.394±0.001 mg/mL). Structure activity relationship was established for tested compounds which revealed that the most active compound **3g** (IC_{50}= 0.383±0.001 mg/mL) possess trifluoromethyl at position 2 of aromatic ring. Compounds **3h** and **3i** possessing trifluoromethyl at position 3 and 4 also exhibited higher antiglycation potential than standard as indicated by their IC_{50} values in Table 3. The glycation inhibition results of the compounds **3g, 3h** and **3i** showed that presence of electron withdrawing groups enhance the ability of compounds to inhibit glycation.

The antiglycation potential of compound **3b** was found similar to standard. The presence of two methoxy group in **3b** at position 4 and 5 and a bromine at position 2 induced potential antiglycation ability. All other compounds were found to have good to excellent antiglycation potential. The electron withdrawing effect of bromine is more pronounced, thus rendering the molecule better antiglycating agent. The electronic effect of groups on glycation inhibition is further supported by the IC_{50} values of compounds **3a** and **3f** where electron donating groups reduce the inhibition potential The results also revealed that glycation inhibition potential is also influenced by the ring size. The presence of five membered ring as **-Ar** group in **3d, 3n** and **3o** possessed lower glycation inhibition potential than standard.

Table 3: Percentage anti-glycation inhibition of compounds **3a-o**.

Compd.	% Age anti-glycation inhibition						IC_{50} (mg/mL±SEM)
	100 ppm	200 ppm	400 ppm	600 ppm	800 ppm	1000 ppm	
3a	62.900	64.266	65.863	66.583	67.892	70.902	0.525±0.005
3b	87.529	88.517	88.725	89.616	90.673	92.144	0.394±0.001
3c	84.679	85.722	86.904	87.235	88.696	90.187	0.404±0.002
3d	70.331	72.396	73.357	74.513	75.128	77.037	0.475±0.003
3e	68.839	72.923	73.403	74.550	75.590	76.629	0.475±0.002
3f	79.391	80.994	86.256	87.982	89.491	91.667	0.402±0.001
3g	90.826	91.158	92.0458	92.805	93.371	93.890	0.383±0.001
3h	90.391	90.781	91.858	92.137	92.546	93.184	0.386±0.001
3i	90.559	91.175	91.877	92.245	92.945	93.783	0.384±0.001
3j	75.108	76.019	80.670	85.752	88.627	89.516	0.414±0.001
3k	82.864	85.201	86.334	87.017	88.296	89.005	0.407±0.002
3l	59.972	67.287	71.121	73.858	78.740	81.663	0.467±0.003
3m	77.707	79.786	82.226	84.116	87.143	88.541	0.417±0.002
3n	83.421	84.699	85.788	87.247	88.782	90.292	0.404±0.001
3o	85.160	87.960	89.099	89.958	91.060	92.267	0.393±0.002
Amino guanidine	86.530	87.572	88.731	89.714	90.684	92.483	0.394±0.001

Structure activity relationship (SAR) for antioxidant potential

The antioxidant potential of compounds **3a-o** was measured by DPPH assay and compared to ascorbic acid. Compounds **3d, 3e, 3j, 3l** and **3m** did not show any significant antioxidant potential. Their percentage antioxidant potential was less than 50 percent hence IC_{50} was not calculated for them. All other compounds **3a, 3b, 3c, 3f, 3g, 3h, 3i, 3k, 3n** and **3o** showed fairly good antioxidant potential but less than standard, their IC_{50} values lie in range 9.34±0.06 to 16.26±0.30 mM. The results presented in the Table 5 revealed that antioxidant potential is dose dependent. All compounds showed minimum potential at minimum tested concentration and maximum antioxidant potential at 15 mM concentration.

The structure activity relationship (SAR) was established for the synthesized compounds and compared to our previously synthesized series of compounds [23]. The SAR studies revealed that antioxidant activity is influenced by nature of groups present on the aryl ring. While comparing results with previous studies it may be concluded that presence of electron donating group (-OMe) enhanced the antioxidant ability of the compounds. This may be evidenced by our current report analogues **3g, 3h** and **3o** (bearing a methoxy group) showed antioxidant activity, when compared with our previously synthesized compounds[23].

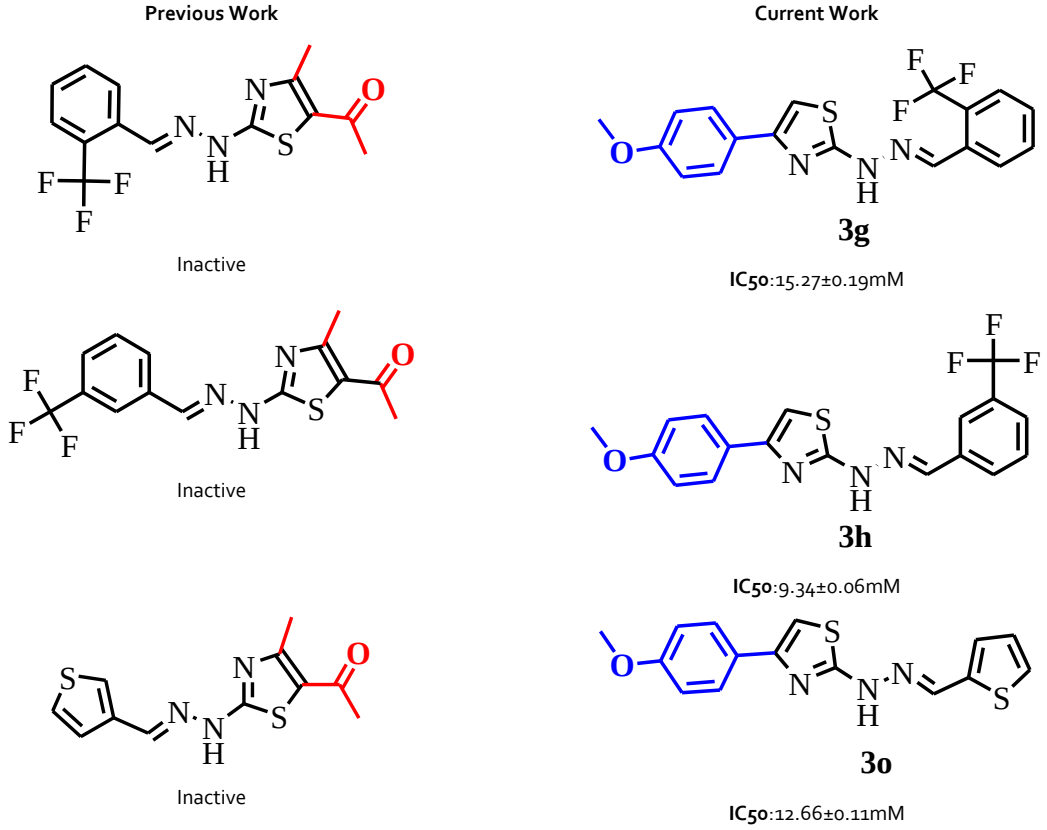

Figure 6: Antioxidant study: Structural comparison of our previous work with our Current work.

These findings are consistent with literature *i.e.,* electron withdrawing groups decrease the antioxidant potential and electron donating groups increase this potential [46]. These electron donating groups easily stabilize and neutralize the DPPH free radical hence, lead to an enhanced antioxidant activity.

Table 4: Percentage antioxidant potential of compounds **3a-o.**

Compd.	% Age antioxidant potential					IC_{50} (mM ±SEM)
	3 mM	6 mM	9 mM	12 mM	15 mM	
3a	0.00	7.09	27.72	51.58	76.32	12.04±0.01
3b	0.00	11.61	31.90	51.55	73.09	11.95±0.01
3c	17.51	26.55	41.34	60.44	72.35	10.34±0.07
3d	0.00	0.00	0.00	11.81	30.19	---
3e	0.00	4.50	8.04	19.58	28.59	---
3f	0.00	12.65	16.06	34.18	62.33	15.81±0.26
3g	0.00	17.55	28.15	37.34	54.56	15.27±0.19
3h	13.85	32.75	44.81	67.46	80.01	9.34±0.06
3i	5.43	20.83	38.88	55.23	65.73	11.57±0.09
3j	0.00	9.54	15.31	25.01	45.35	---
3k	3.82	20.16	33.12	45.24	64.46	12.76±0.15
3l	0.00	0.00	11.27	28.97	43.33	---

3m	0.00	0.00	0.00	0.00	2.74	---
3n	0.00	9.89	16.51	38.88	56.50	16.26±0.30
3o	0.00	13.80	32.22	49.00	66.35	12.66±0.11
Ascorbic Acid	52.54	70.28	77.78	85.26	92.46	6.70±0.01

IC_{50} values: Concentration of the sample (mM) at which DPPH is scavenged by 50%.

In *vitro* haemolytic activity

Compounds **3a-o** were tested for their cytotoxic nature through in *vitro* haemolytic assay and results are presented in Table 6. Compounds **3b, 3d, 3f, 3j** and **3k** were found safe to human erythrocytes at minimum tested concentration. However, at their higher concentrations they induce lysis in human red blood cells (RBCs). Compounds **3e, 3l** and **3n** showed a very minor %age haemolysis at their minimum concentration as indicated in Table 6. The percentage haemolysis of compounds at 10 µM is in following order. **3b=3d=3f=3j=3k<3l<3e<3n<3c<3m<3a<3g<3i<3h<3o**.

Table 5: Percentage haemolysis of the compounds **3a-o**.

Compd.	**% Age haemolysis**		
	10 µM	**50 µM**	**100 µM**
3a	2.53	7.47	32.06
3b	0.00	4.32	8.89
3c	1.12	12.79	32.15
3d	0.00	25.82	44.76
3e	0.98	23.25	49.09
3f	0.00	19.94	39.20
3g	2.95	29.32	52.41
3h	9.06	31.01	49.73
3i	8.35	26.60	36.92
3j	0.00	15.45	36.83
3k	0.00	19.51	37.20
3l	0.90	20.12	42.47
3m	1.25	26.47	40.36
3n	0.99	18.15	41.87
3o	11.54	31.49	51.09
Triton X-100	100	100	100

Conclusions

In present study we have synthesized and studied the α-amylase, glycation inhibition, antioxidant potential and cytotoxicity of 2-(2-arylidenehydrazinyl)-4-(4-methoxyphenyl)thiazoles (**3a-o**). These compounds emerged as potent α-amylase and glycation inhibitor. Among them, **3k** and **3g** were lead α-amylase and glycation inhibitors, respectively. The presence of electron withdrawing groups significantly enhanced the α-amylase and glycation inhibition potential. The antioxidant behavior compared with our previous studies indicated that electron donating groups enhance the antioxidant potential. The behavior of the compounds was found dose dependent in all the biological assays *i.e.* activity increases with increase in concentration. The comparable results of all biological assays are attributed to the same skeleton possessed by compounds. However, effects of substituents was also observed with enhanced or reduced inhibition potential. The cytotoxicity test indicated that this series of compounds is bio-compatible at 10 µM tested concentration. Thus, these compounds may serve as potential lead compounds in diabetes management.

Experimental Section

Material and Methods

All reagents and solvents used in synthesis were of analytical grade. The chemicals were purchased from well reputed suppliers i.e. Sigma Aldrich, Fischer and Acros Organics. Pre-coated thin layer chromatographic (TLC) aluminum sheets (Kiesel gel 60, F_{254}, E. Merck, Germany) were used to monitor the reaction progress and purity of synthesized compounds. Melting points were recorded in open capillaries using DMP-300 A&E Lab, UK, apparatus and are uncorrected. Ultraviolet (UV) absorption spectra were recorded on Shimadzu Ultraviolet-1800 spectrophotometer in DMSO. IR spectra were recorded on Bruker OPUS using ATR to identify the functional groups. The ^{1}H- and ^{13}C-NMR spectra were recorded on Bruker DPX-400 and 500 MHz spectrometer using tetramethyl silane (TMS) as an internal solvent. Mass spectra

were obtained using Bruker Micro TOF-ESI positive targeted mode. Fluorescence of glycated products was measured on Shimadzu RF-6000 spectro-fluorometer.

General procedure for the synthesis of 2-(2-arylidenehydrazinyl)-4-(4-methoxyphenyl)thiazoles (3a-o)

A mixture of aryl substituted thiosemicarbazones (1 mmol) and 2-bromo-4-methoxy acetophenone (1.0 equivalent) was refluxed in absolute ethanol for 4 to 5 hours. The progress of the reaction mixture was monitored at regular intervals with thin layer chromatography. Appearance of single spot at TLC plate indicated the completion of reaction. Upon completion, the reaction mixture was cooled to room temperature and poured on crushed ice. The reaction mixture containing hydrobromic acid (HBr) as side product was neutralized with weak base sodium carbonate (Na_2CO_3). Solid appeared was filtered and washed with plenty of water. TLC pure compounds were obtained upon drying under vacuum with 67-79% yield. The ^{1}H-, and ^{13}C-NMR spectra were run in deuterated dimethyl sufoxide (DMSO-d_6) except **3a, 3b, 3j, 3l** and **3o** which were run in deuterated chloroform ($CDCl_3$). Spectroscopic data of all compounds **3a-o** can be found in supporting information.

Biological assays

α-Amylase inhibition assay

The α-amylase inhibition potential of synthesized compounds was measured by reported protocol [47]. The enzyme and sample mixtures (in 300 µL buffer solution) were incubated at 37 ˚C for 30 minutes in test tubes. A starch solution (Sigma Aldrich, 1% w/v) was prepared in 0.01 M buffer (pH= 6.9) by heating at boiling temperature until clear solution and then cooled to room temperature. A 300 µL starch solution was added to pre-incubated mixtures of enzyme and sample. The reaction mixture was incubated for another 30 minutes. 3,5-Dinitrosalicylic acid (DNSA, 300 µL of a 2 M solution) colour substrate was added and reaction was stopped by placing each test tube immediately in boiling water bath. The test tubes were cooled to room temperature followed by dilution with 1 mL distilled water. To correct the absorbance of coloured test samples a blank was prepared by incubating sample without enzyme solution. A test tube with dimethylsulfoxide (DMSO, 300 µL) without any sample was used as a control. The absorbance of each final solution was recorded with UV-Visible spectrophotometer at 540 nm. Microsoft excel professional plus 2019 software was used to plot the graphs and linear equation was used to calculate the IC_{50} values from the collected data. α-Amylase inhibition was calculated by the formula given below:

Percentage inhibition = [(A control–A sample)/A control]×100

In *vitro* antiglycation assay

Bovine serum albumin (BSA-Glucose) model was used to measure the antiglycation potential of synthesized compounds as reported by khan *et.al.* [48] using amino-guanidine as reference. The assayed mixture contained glucose solution (200 µL, 1.5 mM), BSA (200 µL of 85 mg/mL solution) and 100 µL of the test samples (typically at 1000 ppm, 800 ppm, 600 ppm, 400 ppm, 200 ppm and 100 ppm in dimethylsulfoxide). BSA-Glucose solutions were prepared in phosphate buffer saline (PBS) pH 7.4 and used as control. Sodium azide (0.02% w/v in distilled water) was added as antimicrobial agent. Samples were incubated at 60 °C for two weeks. Trichloroacetic acid (1% w/v) was used to quench the reaction followed by centrifugation at 5000 rpm (7 minute), pellets were formed, separated and re-suspended in PBS. Specific fluorescence intensity (excitation 370 nm; emission 440 nm) was measured to analyze the glycation inhibition. Microsoft excel professional plus 2019 software was used to plot the graphs and linear equation was used to calculate the IC_{50} values from the collected data and percentage inhibition was calculated.

% Inhibition = [(Fluorescence control–Fluorescence sample)/Fluorescence control]×100

DPPH radical scavenging assay

The free radical scavenging ability of the synthesized compounds was evaluated by using 1,1-diphenyl-2-picrylhydrazyl (DPPH) as reported in literature using ascorbic acid as reference [49]. The DPPH solution (1 mM) was prepared in methanol and provided dark environment by wrapping volumetric flask with aluminium foil. Sample solutions were prepared in DMSO ranging from 5 mM to 15 mM. A total of 100 µL of test sample (15 mM, 10 mM and 5 mM) and 900 µL of DPPH (1 mM) were incubated at 37 °C for 30 minutes. The

absorbance was measured at 517 nm by UV-Visible spectrophotometer. DPPH solution without test sample was used as control. Microsoft excel professional plus 2019 software was used to plot the graphs and linear equation was used to calculate the IC_{50} values. Percentage inhibition of radical scavenging potential was calculated by the following formula:

Percentage antioxidant potential = [(Ac–Ai)/Ac] × 100

Ac= Absorbance of control, Ai= Absorbance of sample.

In *vitro* haemolytic assay

In *vitro* haemolytic assay of human erythrocytes was used to determine the cytotoxicity of synthesized compounds. The method reported in the literature was used with some modifications [50]. 20% Triton X-100 was used as positive control induces 100% lysis. 5 mL fresh human blood sample was collected from a healthy volunteer. Blood plasma was removed by centrifuging blood at 7000 rpm for 10 minutes before treatment. The collected erythrocytes were washed three times using phosphate buffer saline (PBS, pH= 7.4). 100 µL of 10 µM, 50 µM or 100 µM samples were added to 900 µL of blood suspension followed by incubation at 37 °C for 30 minutes. The percentage haemolysis was estimated by free haemoglobin present in the supernatant. The absorbance was recorded by UV-Visible spectrophotometer at 540 nm. A blank was made by the supernatant from an untreated erythrocytes suspension with phosphate buffer saline and its absorbance was noted. The experiment was run in triplicate and percent haemolysis was calculated.

%Haemolysis = [(A Sample–A Blank)/(A Control–A Blank)]×100.

Statistical analysis

All biological assays were performed in triplicates and results are presented as mean±SEM from three experiments. The results were analyzed by Microsoft excel professional 2019 software package. IC_{50} values were determined by linear equation.

Molecular modelling Study

In order to validate the biological activity, molecular docking simulations were performed between α-amylase and acarbose or newly synthesized compounds (**3a-o**) using reported literature [23]. All docking studies were performed using Autodock Vina (ver. 1.2.3). For this purpose, the crystal structure of human pancreatic α-amylase complexed with montbretin A (PDB ID: 4W93) were retrieved from protein data bank. The co-crystallized ligand and water molecules were removed and the protein was converted to pdbqt format using Autodock Tools [51] keeping co-factor intact. The 2D structures of ligands were sketched using Chemdraw 12.0. The 2D structures were converted to 3D format by Openbabel (ver. 2.3.1). PDBQT files were prepared in MGL Tools. All the compounds were docked using Autodock Vina. The other parameters were left as default. Finally, the conformations with the most favorable free energy of binding were selected for analyzing the interactions between the target enzyme and inhibitors. The docking scores were obtained as binding energies in Kcal/mol. Discovery Studio (ver. 21.1.0.20298) and UCSF ChimeraX (ver. 1.2) software was used for 3D molecular graphics, structural alignments, and visualizations.

Acknowledgements ((optional))

Author Contribution Statement ((required for publication))

I Dr. Muhammad Haroon confirm that all authors played their role in this work and is briefed as under;

Hasnain Mehmood: Performed the synthetic work and characterized the compounds, Muhammad Haroon: compiled the manuscript. Tashfeen Akhtar: Supervisor of the first author, refined the paper and sharing the correspondence besides being project designer. Simon woodward and Mustapha Musa refined the paper. Muhammad Ehsan and Ehsan Tahir: Docking studies and written that part of the paper as well.

Reference

1. J. A. Al-Lawati, *Oman medical journal*, 2017, **32**, 177.
2. I. D. Federation, *International Diabetes Federation*, 2017, 905-911.
3. A. S. Wagman, R. S. Boyce, S. P. Brown, E. Fang, D. Goff, J. M. Jansen, V. P. Le, B. H. Levine, S. C. Ng and Z.-J. Ni, *Journal of Medicinal Chemistry*, 2017, **60**, 8482-8514.
4. K. Nowotny, T. Jung, A. Höhn, D. Weber and T. Grune, *Biomolecules*, 2015, **5**, 194-222.
5. V. Rani, G. Deep, R. K. Singh, K. Palle and U. C. Yadav, *Life sciences*, 2016, **148**, 183-193.
6. Q. Xu, L. Huang, J. Liu, L. Ma, T. Chen, J. Chen, F. Peng, D. Cao, Z. Yang and N. Qiu, *European journal of medicinal chemistry*, 2012, **52**, 70-81.
7. V. Basavanna, S. Ningaiah, S. Doddamani, U. Bhadraiah, N. Lingegowda and D. Shanthakumar, 2020.
8. M. Taha, N. H. Ismail, W. Jamil, H. Rashwan, S. M. Kashif, A. A. Sain, M. I. Adenan, M. Ali, F. Rahim and K. M. Khan, *European journal of medicinal chemistry*, 2014, **84**, 731-738.
9. A. Adeneye and E. Agbaje, *African Journal of Biomedical Research*, 2008, **11**.
10. M. Kazeem, J. Adamson and I. Ogunwande, *BioMed research international*, 2013, **2013**.
11. O. A. Olajide, S. O. Awe, J. M. Makinde and O. Morebise, *Journal of Pharmacy and Pharmacology*, 1999, **51**, 1321-1324.
12. A. Kumar, P. Kumar and H. Shravya.
13. D. J. Kempf, H. L. Sham, K. C. Marsh, C. A. Flentge, D. Betebenner, B. E. Green, E. McDonald, S. Vasavanonda, A. Saldivar and N. E. Wideburg, *Journal of medicinal chemistry*, 1998, **41**, 602-617.
14. K. D. Hargrave, F. K. Hess and J. T. Oliver, *Journal of medicinal chemistry*, 1983, **26**, 1158-1163.
15. M. T Chhabria, S. Patel, P. Modi and P. S Brahmkshatriya, *Current topics in medicinal chemistry*, 2016, **16**, 2841-2862.
16. T. Sravanthi, S. Sajitha Lulu, S. Vino, M. Jayasri, A. Mohanapriya and S. Manju, *Medicinal Chemistry Research*, 2017, **26**, 1306-1315.
17. S. Kumar, D. Rathore, G. Garg, K. Khatri, R. Saxena and S. K. Sahu, *Int. J. Pharm. Pharm. Sci*, 2017, **9**, 60.
18. S. B. Patchipala, V. R. Pasupuleti, A. V. Audipudi and H. babu Bollikolla, *Arabian Journal of Chemistry*, 2022, **15**, 103546.
19. M. Solangi, K. M. Khan, S. Chigurupati, F. Saleem, U. Qureshi, Z. Ul-Haq, A. Jabeen, S. G. Felemban, F. Zafar and S. Perveen, *Archiv der Pharmazie*, 2022, e2100481.
20. M. F. Arshad, A. Alam, A. A. Alshammari, M. B. Alhazza, I. M. Alzimam, M. A. Alam, G. Mustafa, M. S. Ansari, A. M. Alotaibi and A. A. Alotaibi, *Molecules*, 2022, **27**, 3994.
21. G. L. Khatik, A. K. Datusalia, W. Ahsan, P. Kaur, M. Vyas, A. Mittal and S. K. Nayak, *Current drug discovery technologies*, 2018, **15**, 163-177.
22. U. Salar, K. M. Khan, S. Chigurupati, M. Taha, A. Wadood, S. Vijayabalan, M. Ghufran and S. Perveen, *Scientific reports*, 2017, **7**, 1-17.
23. H. Mehmood, M. Haroon, T. Akhtar, S. Woodward and H. Andleeb, *Journal of Molecular Structure*, 2022, **1250**, 131807.
24. R. Alonso, E. Bermejo, R. Carballo, A. Castiñeiras and T. Pérez, *Journal of molecular structure*, 2002, **606**, 155-173.
25. Y. Fang, M. Xiao, A. Hu, J. Ye, W. Lian and A. Liu, *Chinese Journal of Chemistry*, 2016, **34**, 403-411.
26. X. Chen and Z.-L. Jing, *Acta Crystallographica Section E: Structure Reports Online*, 2011, **67**, 03369-03369.
27. R. Matsa, P. Makam, M. Kaushik, S. Hoti and T. Kannan, *European Journal of Pharmaceutical Sciences*, 2019, **137**, 104986.
28. J. da Silva Santos, J. L. R. de Melos, G. S. Lima, J. C. Lyra, G. P. Guedes, C. E. Rodrigues-Santos and A. Echevarria, *Journal of Fluorine Chemistry*, 2017, **195**, 31-36.
29. P. Linciano, C. B. Moraes, L. M. Alcantara, C. H. Franco, B. Pascoalino, L. H. Freitas-Junior, S. Macedo, N. Santarem, A. Cordeiro-da-Silva and S. Gul, *European Journal of Medicinal Chemistry*, 2018, **146**, 423-434.
30. D. C. Greenbaum, Z. Mackey, E. Hansell, P. Doyle, J. Gut, C. R. Caffrey, J. Lehrman, P. J. Rosenthal, J. H. McKerrow and K. Chibale, *Journal of medicinal chemistry*, 2004, **47**, 3212-3219.
31. K. Hałdys, W. Goldeman, M. Jewgiński, E. Wolińska, N. Anger-Góra, J. Rossowska and R. Latajka, *Bioorganic Chemistry*, 2020, **94**, 103419.
32. S. Bhatia, P. Gautam, A. Chatrath and P. Jain, *Indian journal of chemistry. Sect. B: Organic chemistry, including medical chemistry*, 1993, **32**, 1237-1240.
33. M. Azam, I. Warad, S. I. Al-Resayes, M. R. Siddiqui and M. Oves, *Chemistry & Biodiversity*, 2013, **10**, 1109-1119.
34. T. I. de Santana, M. de Oliveira Barbosa, P. A. T. de Moraes Gomes, A. C. N. da Cruz, T. G. da Silva and A. C. L. Leite, *European journal of medicinal chemistry*, 2018, **144**, 874-886.
35. V. H. Pham, T. P. D. Phan, D. C. Phan and B. D. Vu, *Molecules*, 2020, **25**, 324.
36. M. C. Gidaro, S. Alcaro, D. Secci, D. Rivanera, A. Mollica, M. Agamennone, L. Giampietro and S. Carradori, *Journal of Enzyme Inhibition and Medicinal Chemistry*, 2016, **31**, 1703-1706.
37. A. Taurins, J. Fenyes and R. N. Jones, *Canadian Journal of Chemistry*, 1957, **35**, 423-427.
38. Y. Iqbal, M. Haroon, T. Akhtar, M. Ashfaq, M. N. Tahir, L. Rasheed, M. Yousuf and M. A. Zia, *Journal of Molecular Structure*, 2022, **1267**, 133620.
39. H. Mehmood, M. Khalid, M. Haroon, T. Akhtar, M. Ashfaq, M. N. Tahir, M. U. Khan, M. Imran, A. A. C. Braga and S. Woodward, *Journal of Molecular Structure*, 2021, **1245**, 131043.
40. M. Haroon, T. Akhtar, M. Khalid, S. S. Zahra, I.-u. Haq, M. A. Assiri, M. Imran and A. A. Braga, *Journal of Molecular Structure*, 2022, **1270**, 133923.
41. M. Haroon, T. Akhtar, M. Yousuf, M. N. Tahir, L. Rasheed, S. S. Zahra and M. Ashfaq, *BMC chemistry*, 2022, **16**, 1-17.
42. M. Haroon, M. Khalid, T. Akhtar, M. N. Tahir, M. U. Khan, S. Muhammad, A. G. Al-Sehemi and S. Hameed, *Journal of Molecular Structure*, 2020, **1202**, 127354.
43. M. Haroon, M. Khalid, K. Shahzadi, T. Akhtar, S. Saba, J. Rafique, S. Ali, M. Irfan, M. M. Alam and M. Imran, *Journal of Molecular Structure*, 2021, **1245**, 131063.
44. M. Haroon, M. C. H. de Barros Dias, A. C. da Silva Santos, V. R. A. Pereira, L. A. B. Freitas, R. B. Balbinot, V. Kaplum, C. V. Nakamura, L. C. Alves and F. A. Brayner, *RSC advances*, 2021, **11**, 2487-2500.
45. M. Haroon, T. Akhtar, M. Khalid, S. Ali, S. Zahra, M. Alhujaily, M. C. d. B. Dias, A. C. L. Leite and S. Muhammad, *Zeitschrift für Naturforschung C*, 2021, **76**, 467-480.

46. C. Y. Lee, C. Anamoah, J. Semenya, K. N. Chapman, A. N. Knoll, H. F. Brinkman, J. I. Malone and A. Sharma, *Tetrahedron Letters*, 2020, **61**, 151607.
47. P. P. McCue and K. Shetty, *Asia Pacific Journal of Clinical Nutrition*, 2004, **13**.
48. S. D. Sharma, B. Pandey, K. Mishra and S. Sivakami, *J Biochem Mol Biol Biophys*, 2002, **6**, 233-242.
49. R. Suthakaran, G. Somasekhar, C. Sridevi, M. Marikannan, K. Suganthi and G. Nagarajan, *Asian Journal of Chemistry*, 2007, **19**, 3353.
50. D. Malagoli, *Invertebrate Survival Journal*, 2007, **4**, 92-94.
51. M. F. Sanner, *J Mol Graph Model*, 1999, **17**, 57-61.

Entry for the Graphical Illustration ((required for publication))

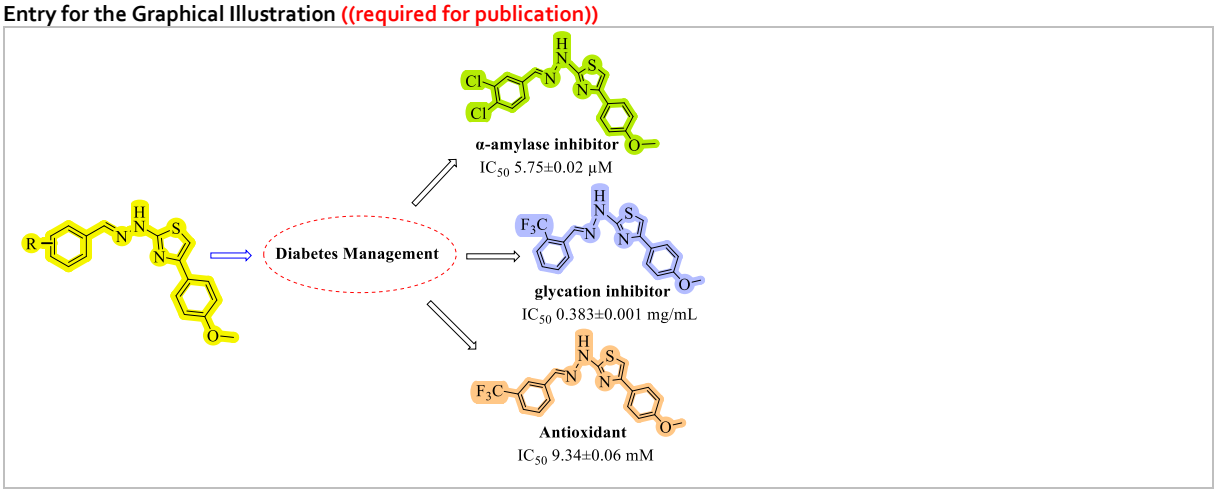

Twitter Text

- A convenient synthesis of the Arylidenehydrazinyl-4-methoxyphenylthiazole Derivatives accomplished in three steps.
- Confirmation of synthesis achieved *via* UV, FT-IR, NMR and Mass spectrometric techniques.
- Antiglycation, amylase and antioxidant experimental and docking results of almost all tested compounds are comparable to standard.